Analysis of Diffusion in Polymers Using Evanescent Field Spectroscopy

Gregory T. Fieldson and Timothy A. Barbari
Dept. of Chemical Engineering, Johns Hopkins University, Baltimore, MD 21218

A rigorous analysis confirmed by experimental results is presented for attenuated total reflectance, Fourier-transform infrared (FTIR-ATR) spectroscopy applied to the study of small molecule diffusion in polymers. FTIR-ATR Fickian diffusion models are derived for a constant surface concentration and for an adjacent mass-transfer boundary layer. An FTIR-ATR Case II transport model demonstrates the ability to discriminate between transport modes. New experimental results for the acetone-polypropylene, methanol-polystyrene and methanol-poly(methyl methacrylate) systems are consistent with gravimetric sorption and nuclear magnetic resonance measurements. An important result is the detection of multiple hydroxyl peaks for methanol during diffusion, indicating different hydrogen bonding states and the calculation of separate diffusion coefficients for each state in polystyrene.

Introduction

In polymer science, most applications of evanescent field spectroscopy, namely attenuated total reflectance, Fourier transform infrared (FTIR-ATR) spectroscopy and total internal reflectance fluorescence (TIRF) spectroscopy, have been related to surface characterization. However, there has been an increasing number of investigations that use FTIR-ATR spectroscopy for studying diffusion in polymers. Vorenkamp et al. (1989) suggested that interdiffusion of poly(vinyl chloride) and poly(methyl methacrylate) could be monitored with FTIR-ATR spectroscopy. They observed an increase of the carbonyl stretching band absorbance of poly(methyl methacrylate) diffusing in poly(vinyl chloride), but they did not calculate a diffusion coefficient. Diffusion models were applied to polymer-polymer interdiffusion in FTIR-ATR spectroscopy by Van Alsten and Lustig (1992) with polystyrene and poly(methyl methacrylate) by Lustig et al. (1993) with poly(ether imide) and poly(aryl ether ketone ketone), and by Jabbari and Peppas (1992) with polystyrene and poly(vinyl methyl ether).

FTIR-ATR spectroscopy was first applied to small molecule diffusion in polymers by Schlotter and Furlan (1992). They studied the diffusion of additives in polyolefins and attempted to relate the absorbance of additives to their mass uptake. Using a somewhat different mathematical approach, Fieldson and Barbari (1993) integrated the concentration profile with the intensity of the evanescent field to obtain an analytical solution to the problem of one-dimensional (1-D) Fickian diffusion with a constant surface concentration. They derived a simplified form of the FTIR-ATR Fickian diffusion model at long times, and applied this model to diffusion results for the water-polyacrylonitrile system.

In this article, the FTIR-ATR Fickian diffusion model (Fieldson and Barbari, 1993) is generalized to incorporate the effect of an adjacent mass-transfer boundary layer. A simple model for studying Case II diffusion in FTIR-ATR spectroscopy is also derived and the ability to discriminate between diffusion modes is demonstrated. New experimental results which demonstrate the capabilities of FTIR-ATR spectroscopy are presented. Systems that are studied include the diffusion of acetone in polypropylene, methanol in polystyrene and methanol in poly(methyl methacrylate).

Theoretical Development

FTIR-ATR spectroscopy

When light is reflected at an interface with a rarer medium, an evanescent wave exists in this adjacent phase. The evanescent wave is characterized by an electric field magnitude which decays exponentially with distance from the interface. The rate of decay is dependent on the refractive indices of

Correspondence concerning this article should be addressed to T. A. Barbari.

the two media, the angle of incidence, and the wavelength of the light. The change in the electric field, E, from its value at the interface, E_0, is given by (Mirabella, 1993):

$$E = E_0 e^{-\gamma z} \tag{1}$$

where γ is the evanescent field decay coefficient, and is a function of the optical parameters of the system defined as (Mirabella, 1993):

$$\gamma = \frac{2n_2\pi\sqrt{\sin^2\theta - \left(\frac{n_1^2}{n_2^2}\right)}}{\lambda} \tag{2}$$

In Eq. 2, n_1 and n_2 are the refractive indices of the rarer and propagating media, respectively, θ is the angle of incidence, and λ is the wavelength of the light in free space.

If the adjacent medium is capable of absorbing light at some frequency present in the evanescent wave, this energy is removed from the reflected wave. This absorbance can be detected by either measuring a decrease in the reflected wave intensity (absorption spectroscopy), or by measuring light emitted in the adjacent medium (fluorescence spectroscopy).

The absorbance of light is related to the intensity of the electric field I which is equal to the square of the electric field magnitude.

The reciprocal of γ is referred to as the depth of penetration d_p. This is the distance from the interface at which the electric field intensity is $1/e^2$, or 13%, of its value at the interface, E_0^2. Figure 1 shows the relationship between the intensity of the evanescent field and distance from the reflecting interface for several values of γ.

When infrared light is reflected at an appropriate interface, the evanescent field is absorbed by dipoles in the adjacent medium. The reflected light is directed to a detector and the resulting spectrum is similar to that obtained in transmission IR spectroscopy. Due to the low level of light ultimately reaching the detector, Fourier transform infrared spectrometers are usually necessary. This technique is called attenuated total reflectance, Fourier transform infrared, or FTIR-ATR spectroscopy. The general expression for absorbance in FTIR-ATR spectroscopy for weak absorbers (Tompkins, 1974) is:

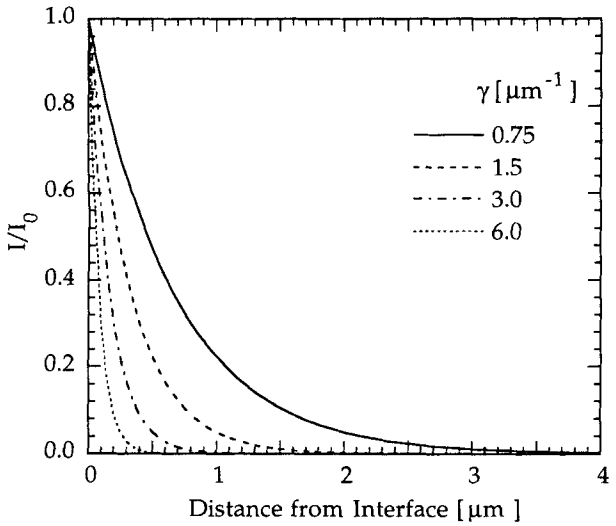

Figure 1. Evanescent field intensity as a function of distance from the interface.

$$A = \int_0^L \epsilon^* C e^{-2\gamma z} dz \tag{3}$$

where ϵ^* is a constant which includes the refractive indices, the molar extinction coefficient, the number of reflections and the cross-sectional area of the infrared beam, and C is the concentration of an absorbing group. When γ is constant, this reduces to the expression that has been previously applied (Fieldson and Barbari, 1993).

If the absorbing group is associated with a diffusing penetrant, a concentration profile can be substituted into Eq. 3 and the result integrated to obtain an expression for the absorbance as a function of time. This analysis assumes that the change in refractive index with concentration is small (dilute system). For strong absorbers and high concentrations, the refractive index of the absorbing medium must include the imaginary component to correct for optical distortion and the dependence on concentration, respectively.

Fickian diffusion, constant surface concentration

For 1-D molecular diffusion in a film with a constant diffusion coefficient, the combination of Fick's law and the continuity equation for the penetrant is:

$$\frac{\partial C}{\partial t} = D\frac{\partial^2 C}{\partial z^2} \tag{4}$$

where C is the concentration of penetrant and D is the diffusion coefficient. Equation 4 can be readily solved, given the appropriate boundary conditions. Figure 2 shows the arrangement of a polymer film adjacent to an internal reflection element (IRE) with a fluid flowing past the opposite surface of the film. The initial and boundary conditions for the case of constant surface concentration are:

$$C = 0 \quad \text{at } t < 0;\ 0 \le z \le L$$
$$C = C_L \quad \text{at } t \ge 0;\ z = L$$
$$\frac{\partial C}{\partial z} = 0 \quad \text{at } t \ge 0;\ z = 0$$

One solution to Eq. 4 with these boundary and initial conditions is:

$$\frac{C}{C_L} = 1 - \frac{4}{\pi}\sum_{n=0}^{\infty}\frac{(-1)^n}{2n+1}\exp\left[\frac{-D(2n+1)^2\pi^2 t}{4L^2}\right] \times\cos\left[\frac{(2n+1)\pi z}{2L}\right] \tag{5}$$

When the refractive index of the polymer is assumed constant, Eqs. 3 and 5 can be combined and integrated to pro-

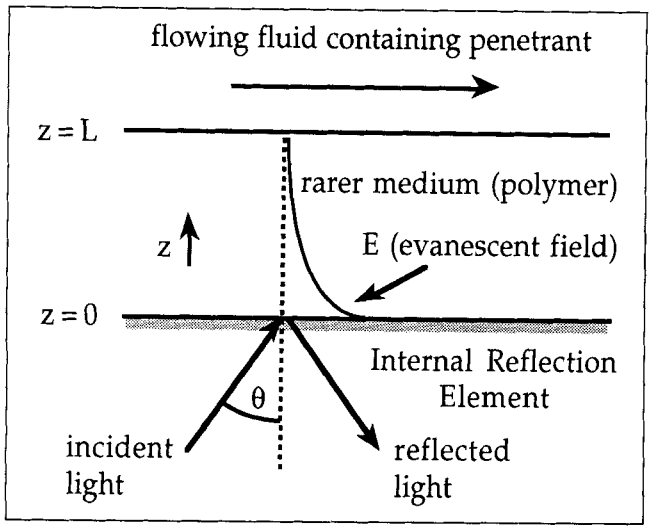

Figure 2. Experimental configuration for studying diffusion in polymers with FTIR-ATR spectroscopy.

vide an expression for the ratio of absorbance at any time A to that at equilibrium A_∞ (Fieldson and Barbari, 1993). This expression is:

$$\frac{A}{A_\infty} = 1 - \frac{8\gamma}{\pi(1-e^{-2\gamma L})} \sum_{n=0}^{\infty} \frac{e^g(fe^{-2\gamma L} + (-1)^n(2\gamma))}{(2n+1)(4\gamma^2 + f^2)} \quad (6)$$

where

$$f = \frac{(2n+1)\pi}{2L}$$

and

$$g = \frac{-D(2n+1)^2\pi^2 t}{4L^2}$$

Equation 6 is analogous to the mass uptake expression for gravimetric sorption. An approximation of this equation at long times was derived and used by Fieldson and Barbari (1993) to test the applicability of FTIR-ATR spectroscopy for studying diffusion in polymers. The approximation presented in that article allowed a clear parallel to be drawn between the FTIR-ATR measurements of diffusion and gravimetric sorption measurements. The use of this approximation is neither necessary nor advantageous, however, and the complete FTIR-ATR Fickian diffusion model for constant surface concentration (Eq. 6) is used below to regress experimental data.

As with gravimetric sorption measurements, the regression of experimental results with Eq. 6 necessarily yields a diffusion coefficient that is averaged over the experimental concentrations. In cases where D may be explicitly expressed as a function of concentration, it is possible to reformulate Eq. 4 and ultimately derive an expression analogous to Eq. 6.

Fickian diffusion, mass-transfer boundary layer in adjacent phase

If the polymer sorbs a single penetrant from a liquid mixture, the concentration of the penetrant in the liquid at the polymer-liquid interface may not be the same as the concentration in the bulk liquid. In this case, it is necessary to account for mass transfer through the boundary layer adjacent to the surface of the film. The initial and boundary conditions for this problem are:

$$C = 0 \qquad \text{at } t < 0;\ 0 \le z \le L$$

$$-D\frac{\partial C}{\partial z} = \frac{k_c}{K}(KC_b - C) \qquad \text{at } t \ge 0;\ z = L$$

$$\frac{\partial C}{\partial z} = 0 \qquad \text{at } t \ge 0;\ z = 0$$

where k_c is the mass-transfer coefficient for the adjacent liquid phase, K is the equilibrium partition coefficient between the polymer and the liquid, and C_b is the bulk concentration of penetrant in the liquid phase.

An analytical solution for the concentration of penetrant in the polymer during unsteady-state diffusion with the above boundary conditions is:

$$\frac{C}{KC_b} = 1 - \sum_{n=1}^{\infty} \frac{2\alpha \cos\left(\beta_n \frac{z}{L}\right)}{(\beta_n^2 + \alpha^2 + \alpha)\cos\beta_n} \exp\left(\frac{-\beta_n^2 Dt}{L^2}\right) \quad (7)$$

where

$$\alpha = \frac{k_c L}{KD}$$

and the β_ns are the solutions of:

$$\alpha = \beta_n \tan\beta_n$$

Assuming the refractive index is constant, Eq. 7 can be combined with the FTIR-ATR absorbance equation (Eq. 3) and integrated, yielding:

$$\frac{A}{A_\infty} = 1 - \frac{4\gamma\alpha}{(1-e^{-2\gamma L})} \sum_{n=1}^{\infty} \exp\left(\frac{-\beta_n^2 Dt}{L^2}\right) \times \frac{\cos(\beta_n)e^{-2\gamma L}\left(\frac{\alpha}{L} - 2\gamma\right) + 2\gamma}{(\beta_n^2 + \alpha^2 + \alpha)\left(4\gamma^2 + \frac{\beta_n^2}{L^2}\right)\cos(\beta_n)} \quad (8)$$

Equation 8 is a more general form of the FTIR-ATR absorbance model for Fickian diffusion. Equation 6 can be recovered from Eq. 8 by setting $\alpha = \infty$.

The effect of the boundary layer resistance upon the absorbance measured in FTIR-ATR spectroscopy can be explored by evaluating Eq. 8 at different values of α. Figure 3a shows a series of absorbance curves corresponding to values of α of 0.1, 1, 2, 10, and ∞. It is clear that the boundary layer resistance will reduce the rate at which penetrant is sorbed. The results can be plotted, as in Figure 3b, with the dimen-

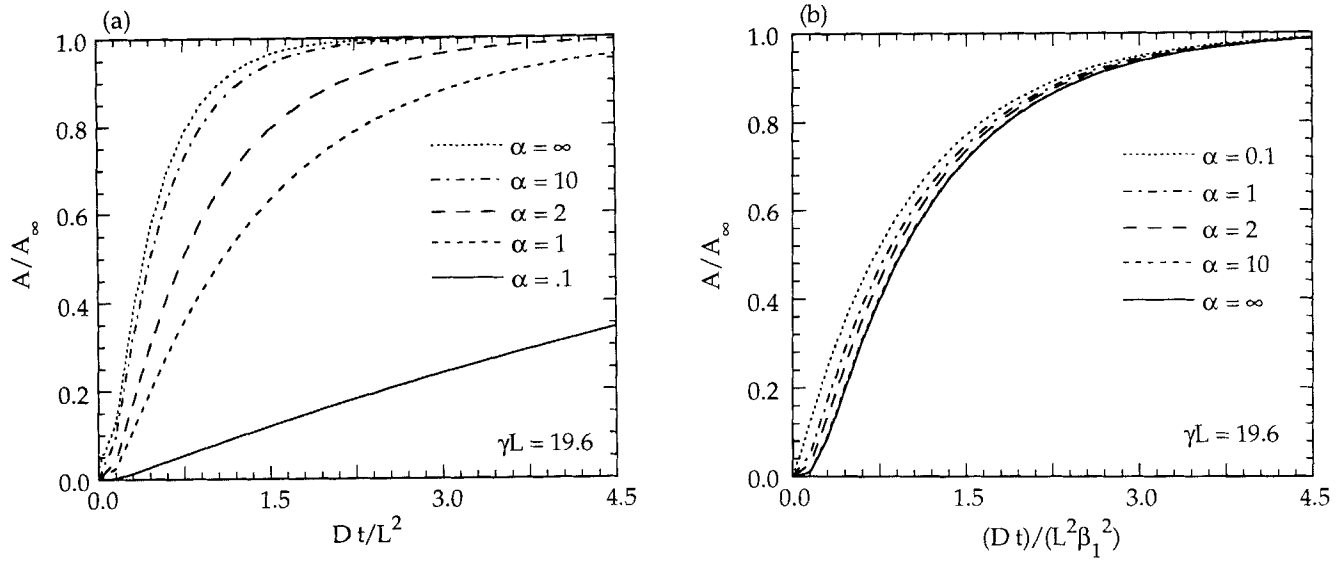

Figure 3. Absorbance ratios for the mass-transfer boundary layer FTIR-ATR Fickian diffusion model.

(a) As function of dimensionless time; (b) as function of dimensionless time scaled by $1/\beta_1^2$.

sionless time divided by β_1^2. This figure reveals that, while at long times the curves become coincident, they are not superimposable.

Case II diffusion, constant surface concentration, constant velocity front

The exploration of various models of Case II diffusion and their incorporation into the mathematics of evanescent field spectroscopy is beyond the intent of this article. There are numerous descriptions of this transport process, unique to polymers, in the literature (Adib and Neogi, 1987; Alfrey et al., 1966; Camera-Roda and Sarti, 1990; Neogi, 1983; Thomas and Windle, 1982; Windle, 1985). Here, the simplest description of Case II transport is applied in order to reveal the main features of the absorbance curves, and to contrast the FTIR-ATR absorbance of Case II transport with that of Fickian diffusion.

The simplest description of a penetrant following Case II diffusion is a constant penetrant concentration front which moves from the polymer-penetrant interface into the polymer film with a constant velocity v (Alfrey et al., 1966). The concentration profile for this expression, as a function of position and time can be described by:

$$C(z,t) = C_L \mathcal{H}(z + vt - L) \tag{9}$$

where

$\mathcal{H}(x)$ = the Heaviside function:

$$\mathcal{H}(x < 0) = 0$$
$$\mathcal{H}(x \geq 0) = 1$$

This concentration profile can be substituted into Eq. 3 and integrated to give:

$$\frac{A}{A_\infty} = \frac{1 - e^{2\gamma vt}}{1 - e^{2\gamma L}} \tag{10}$$

for

$$\frac{vt}{L} \leq 1$$

A plot of A/A_∞ as a function of time for several values of γL is shown in Figure 4. According to this simple model for Case II diffusion, equilibrium occurs when the dimensionless time, vt/L, reaches unity. The front velocity is calculated by simply dividing the initial thickness of the polymer sample L by the time required to reach the equilibrium absorbance. A unique and characteristic behavior of Case II diffusion is that A/A_∞ approaches unity in an exponential manner. Figure 5 shows a comparison of the predicted FTIR-ATR Case II diffusion absorbance (Eq. 10) with the FTIR-ATR Fickian dif-

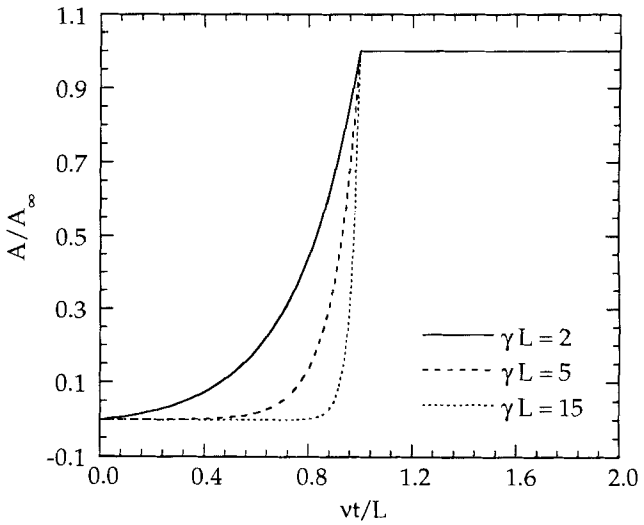

Figure 4. Absorbance ratio for the simple FTIR-ATR Case II model.

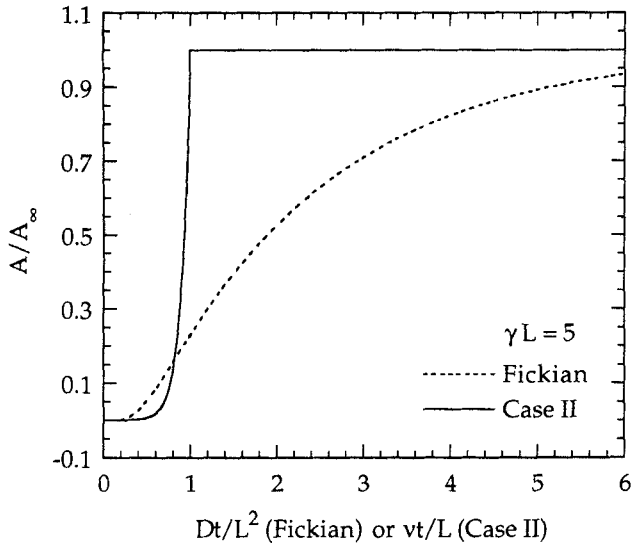

Figure 5. Absorbance ratios for FTIR-ATR Fickian diffusion and Case II diffusion models.

fusion absorbance (Eq. 6). This figure suggests that the two modes of diffusion should be easily differentiated in FTIR-ATR spectroscopy.

Experimental

FTIR-ATR spectroscopy was used to investigate the diffusion of methanol in polystyrene and in poly(methyl methacrylate) and the diffusion of acetone in polypropylene. The experimental procedure for applying FTIR-ATR spectroscopy to the study of diffusion was executed as previously reported (Fieldson and Barbari, 1993). The conditions and optical parameters for the three experimental systems are listed in Table 1.

The polypropylene (Shell WRD5 1015) was obtained as an extruded film from Shell Development Company, and was hot pressed onto a silicon internal reflection element (IRE) for testing. The percent crystallinity of the polypropylene was 59%, as reported by Shell. The polystyrene (Dow Styron) was spin coated from a solution of toluene onto a silicon IRE. The poly(methyl methacrylate) sample (Aldrich 18,224-9) was spin coated from toluene. The methanol (Fisher A935-4) and acetone (J. T. Baker 9006-03) used as penetrants in these studies were of spectrophotometric grade.

The analysis and regression of the experimental results proceeded in a manner slightly different from our earlier FTIR-ATR studies. The first important change involved the method used to measure the area of absorbance peaks in the sample spectra. In most of this work, a peak fitting algorithm in the spectrometer software, Advanced FIRST (Mattson Instruments, Inc.), was used to fit synthetic Gauss-Lorentz sum peaks to the experimental data. The area of these synthetic peaks was directly calculated and reported as the integrated absorbance. This method is often better than direct numerical integration of the infrared data, because it allows for the deconvolution of overlapping peaks. The second change was the form of the FTIR-ATR model with which the experimental data were regressed. In this work, either the complete FTIR-ATR Fickian diffusion model with constant surface concentration (Eq. 6) or the simple Case II model (Eq. 10) was regressed to the experimental data using a Levenberg-Marquardt minimization algorithm that is incorporated in MathCAD. The confidence intervals reported for these experiments were calculated according to the description of Sen and Srivastava (1990). Confidence intervals reported for any nonlinear regression are inherently less meaningful, but the FTIR-ATR Fickian diffusion model does not possess any singularities or strong nonlinearities in the region of interest, so these results are fairly robust.

Confirmation of the FTIR-ATR results was obtained by gravimetric sorption measurements for the acetone-polypropylene and methanol-polystyrene systems. The measurements were conducted on polymer samples weighing approximately 1 gram that were dried under vacuum for several days prior to use. The polymer film was weighed, immersed in penetrant, and then periodically removed, blotted and reweighed. Measurements were made on a Mettler AE100 balance that has an accuracy of ± 100 μg. Analysis of the data was done using the standard short-time gravimetric sorption analysis, as described by Crank (1975).

Results and Discussion

Fickian diffusion

Acetone in Polypropylene. The diffusion of acetone in polypropylene (PP) is a simple demonstration system which does not possess any specific interactions between the polymer and the penetrant. At the experimental temperature 20°C, polypropylene is in a semicrystalline rubbery state, and Fickian diffusion of acetone is expected. The presence of acetone in the polypropylene film was measured through the carbonyl bond stretching absorbance located at 1,718 cm^{-1}. A series of infrared spectra of the carbonyl absorbance of acetone in polypropylene is shown in Figure 6. The area of the acetone absorbance peak is plotted in Figure 7. The regressed diffusion coefficient of acetone in PP is 5.23×10^{-10} cm^2/s, and the 99% confidence intervals are 4.98 to 5.49×10^{-10} cm^2/s. The value of A_∞ was obtained by regression of

Table 1. Experimental Conditions and Optical Parameters for Diffusion Experiments

Polymer	Polypropylene	Polystyrene	Poly(methyl methacrylate)	
Penetrant	Acetone	Methanol	Methanol	Methanol
Thickness	28 μm	19 μm	7.8 μm	14.8 μm
Temperature	20°C	23°C	20°C	35°C
n_1	1.49	1.59	1.49	1.49
Sample time	4.83 min	0.29 min	0.15 min	0.29 min
γL	24	20–26	13	25

Common conditions: silicon IRE, $\Theta = 30°$, $n_2 = 3.4$, FTIR resolution = 4 cm^{-1}.

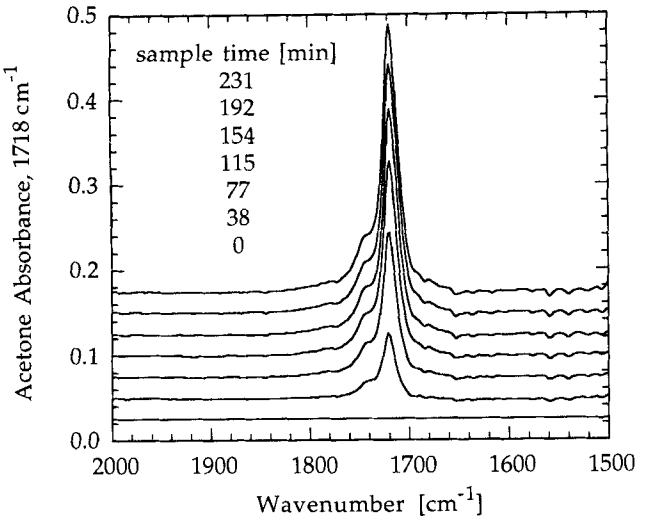

Figure 6. Carbonyl region of the infrared spectra of acetone diffusing in polypropylene at 20°C.

the experimental data and is 7.856, with a 99% confidence interval of 7.66 to 8.08. The absorbance curves for the regressed FTIR-ATR Fickian diffusion model (Eq. 6) and the 99% confidence intervals are included in Figure 7.

A 1-D Fickian diffusion model was used here to describe transport in the semicrystalline polypropylene. Crystalline regions in a polymer are generally regarded as impermeable (Rogers, 1985). As a result, diffusion in semicrystalline materials is best described as transport along a tortuous path in the amorphous fraction. A basic relationship between the overall diffusion coefficient D as measured here, and the diffusion coefficient in the amorphous fraction is:

$$D = D_a \phi_a^m \tag{11}$$

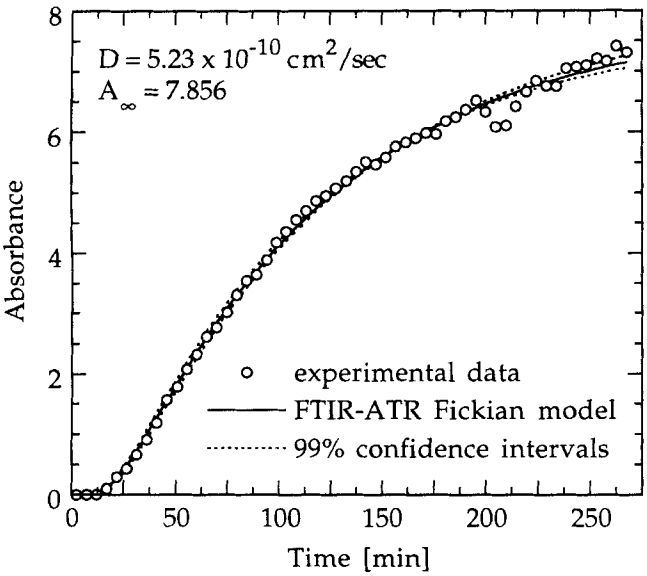

Figure 7. Integrated carbonyl absorbance as a function of time for acetone diffusing in polypropylene at 20°C.

where D_a is the diffusion coefficient for the amorphous material, ϕ_a is the amorphous fraction and m is an empirical parameter. Reported values of m range from about 0.3 in polyethylene to near unity for polyethylene terephthalate (Rogers, 1985); the value of m depends on the geometry of the crystalline regions. Reporting the results in terms of an overall diffusion coefficient instead of an amorphous diffusion coefficient allows direct comparison with other PP samples of similar percent crystallinity, but a value of m is necessary to apply these results more generally.

To our knowledge, a diffusion coefficient for acetone in polypropylene at 20°C has not been reported. Using the "pat and weigh" gravimetric technique described above at room temperature, 23°C, a diffusion coefficient of 5.35×10^{-10} cm^2/s was measured. However, the 95% confidence interval of the diffusion coefficient was 0.7 to 11.2×10^{-10} cm^2/s. The primary sources of error in the diffusion coefficient measured by gravimetric sorption are the limited number of sample points, the small quantity of acetone sorbed by the polymer sample, and the uncertainties inherent in removing excess solvent from the surfaces. The diffusion coefficient measured by gravimetric sorption is averaged over short times, and thus low penetrant concentrations, while the FTIR-ATR diffusion coefficients are averaged over all penetrant concentrations. Even so, the similarity between the gravimetric sorption and FTIR-ATR diffusion results for acetone in polypropylene demonstrates the basic validity and effectiveness of FTIR-ATR spectroscopy for investigating the diffusion of small molecules in polymer films.

Methanol in Polystyrene. The diffusion of methanol in polystyrene (PS) is slightly more complex than that of acetone in polypropylene. At the experimental temperature of 23°C, polystyrene is in an amorphous glassy state. There are also hydrogen bonding interactions which can occur between methanol molecules and between methanol and the phenyl ring attached to the polymer chain. The presence of methanol in the polystyrene is quantified by measuring the hydroxyl stretching absorbances. The location of these absorbance peaks is dependent on the hydrogen bonding, and the molar absorption coefficient for the different hydrogen bonding states is not constant. A second, independent measurement of the total methanol concentration was possible through the CH stretching absorbance, located at 2,830 cm^{-1}, which is assigned to methyl CH. This peak is not subject to any detectable shifting or alteration caused by hydrogen bonding.

The infrared spectra of methanol diffusing in polystyrene are shown in Figure 8. In this figure, it is quite evident that the stretching absorbance of the methanol hydroxyl group occurs at two distinct locations. A large absorbance peak for methanol occurs at 3,350 cm^{-1}, and a smaller peak is located at 3,607 cm^{-1}. The methyl absorbance peak at 2,830 cm^{-1} is also visible, but it is apparent that other CH absorbances interfere with this peak. This interference makes quantification of the methyl CH peak less accurate than the OH stretching peaks.

The absorbance spectra of several methanol standards in toluene, an analog of polystyrene, and in carbon tetrachloride, an inert solvent, were recorded in addition to methanol in polystyrene. From these standards, peak assignments for the OH stretching absorbances of methanol in polystyrene were made. Unassociated methanol, present in low concen-

trations in CCl_4, absorbs at 3,643 cm^{-1}, whereas low concentrations of methanol in toluene and polystyrene absorb at 3,607 cm^{-1}. The shift is the result of weak hydrogen bonding between the methanol dipole and the slightly polar phenyl ring (Reilly, 1993). This methanol peak is referred to as monomeric methanol in the discussion below. At higher concentrations in toluene, CCl_4 and polystyrene, the dominant methanol peak is located at 3,350 cm^{-1}. This absorbance is assigned to methanol that is self-associated through hydrogen bonding. From the absorbance data of methanol in toluene, it is also possible to calculate the molar absorption coefficients, and convert the absorbance of methanol into concentration data. While this conversion is exactly correct when the methanol concentration is constant throughout the polymer, it can also be applied to diffusing systems with negligible error when the value of γL is sufficiently large. For the values of γL in this experiment, which vary from 20 to 26, the substitution of concentration at $z = 0$ for absorbance is made without introducing any significant error.

Figure 9 shows the concentration of methanol as a function of time for the different absorbance peaks. The concentrations of monomeric and self-associated methanol are plotted in Figures 9a and 9b, respectively. Figure 9c plots the total concentration of methanol, as calculated by the addition of the monomeric and self-associated methanol concentrations. Figure 9d plots the absorbance of the methyl CH stretch, an alternative measure of the total methanol concentration. The absorbance curves for the regressed fit of the FTIR-ATR Fickian diffusion model and the 99% confidence interval are also included in these figures.

The two distinct peaks in the methanol OH absorption suggest that there are two significant methanol states, and that the shift between these states is the result of differences in hydrogen bonding. The transition between hydrogen bonding states may be described by a chemical equilibrium reaction (Prausnitz et al., 1986). The diffusion of methanol in polystyrene, with two penetrant states assumed to be in local equilibrium, is essentially identical to the dual mode transport model for gases in glassy polymers. The mathematical similarity between dual mode and coupled diffusion-reaction models has been previously recognized (Vieth, 1991). Applying an important result of the dual mode model under conditions of local equilibrium, the transport of methanol can be described as two diffusing states, monomeric and self-associated, with seemingly independent diffusion coefficients.

The values of C_L and A_∞, which are shown in Figures 9a–9d, were calculated from the average absorbances at long times. Therefore, the diffusion coefficient D is the only parameter regressed in the FTIR-ATR Fickian diffusion model (Eq. 6). The regressed diffusion coefficient for the monomeric methanol is 0.84×10^{-8} cm^2/s with a 99% confidence interval of 0.78 to 0.89×10^{-8} cm^2/s. The diffusion coefficient of self-associated methanol is 2.65×10^{-8} cm^2/s with a 99% confidence interval of 2.22 to 3.21×10^{-8} cm^2/s. The diffusion coefficients for the total methanol, as measured by the sum of the methanol OH stretching concentrations and from the methyl group absorbance, are 1.60 and 1.18×10^{-8} cm^2/s with confidence intervals of 1.41 to 1.82 and 0.98 to 1.44×10^{-8} cm^2/s, respectively. As in the case of the acetone-polypropylene system, no reported values for the diffusion coefficient of methanol in polystyrene were found in the literature.

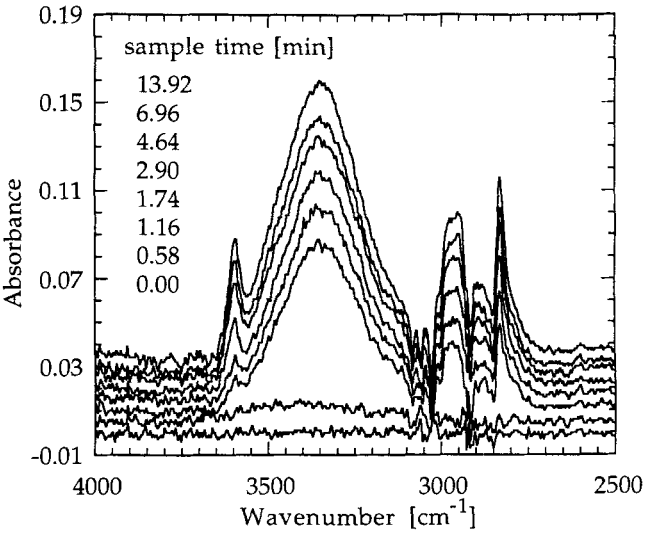

Figure 8. Infrared spectra of methanol diffusing in polystyrene at 23°C.

"Pat and weigh" gravimetric sorption experiments were conducted at 23°C on polystyrene samples to obtain an independent measurement of the diffusion coefficient. As a result of a greater total penetrant uptake, the gravimetric sorption measurement of methanol in polystyrene was more accurate than that of acetone in polypropylene. The diffusion coefficient was 0.85×10^{-8} cm^2/s with a 99% confidence interval of 0.73 to 1.01×10^{-8} cm^2/s, a range which overlaps that for the diffusion coefficient measured by FTIR-ATR spectroscopy using the methyl CH stretch.

The diffusion results for methanol in polystyrene also confirm the basic ability of FTIR-ATR spectroscopy to measure diffusion coefficients. These results demonstrate the unique capabilities of FTIR-ATR spectroscopy for diffusion studies. In this experiment, interactions between the polymer and penetrant, and between penetrant molecules were revealed through the hydrogen bonding of methanol. Diffusing methanol exists in the polymer in two states, a monomeric state, in which the penetrant is weakly associated with the polymer, and a self-associated state. Furthermore, the diffusion coefficients for each of these states were different. The higher apparent diffusion coefficient for the self-associated methanol may reflect an anomalous transport mechanism. Such mechanisms, including Case II diffusion, are observed often in glassy polymers. The presence of two diffusing methanol states implies that the transport of methanol in polystyrene is not a simple binary process. The observation of both monomeric and self-associated methanol with separate diffusion coefficients suggests the use of a dual mode transport model and work is presently underway to further investigate multistate diffusion.

Case II diffusion

Methanol in Poly(methyl methacrylate). The diffusion of methanol in PMMA is a classic example of Case II diffusion (Windle, 1985). The presence of methanol in PMMA was quantified by measuring the absorbance of the hydroxyl group of methanol. The transport of methanol in PMMA was stud-

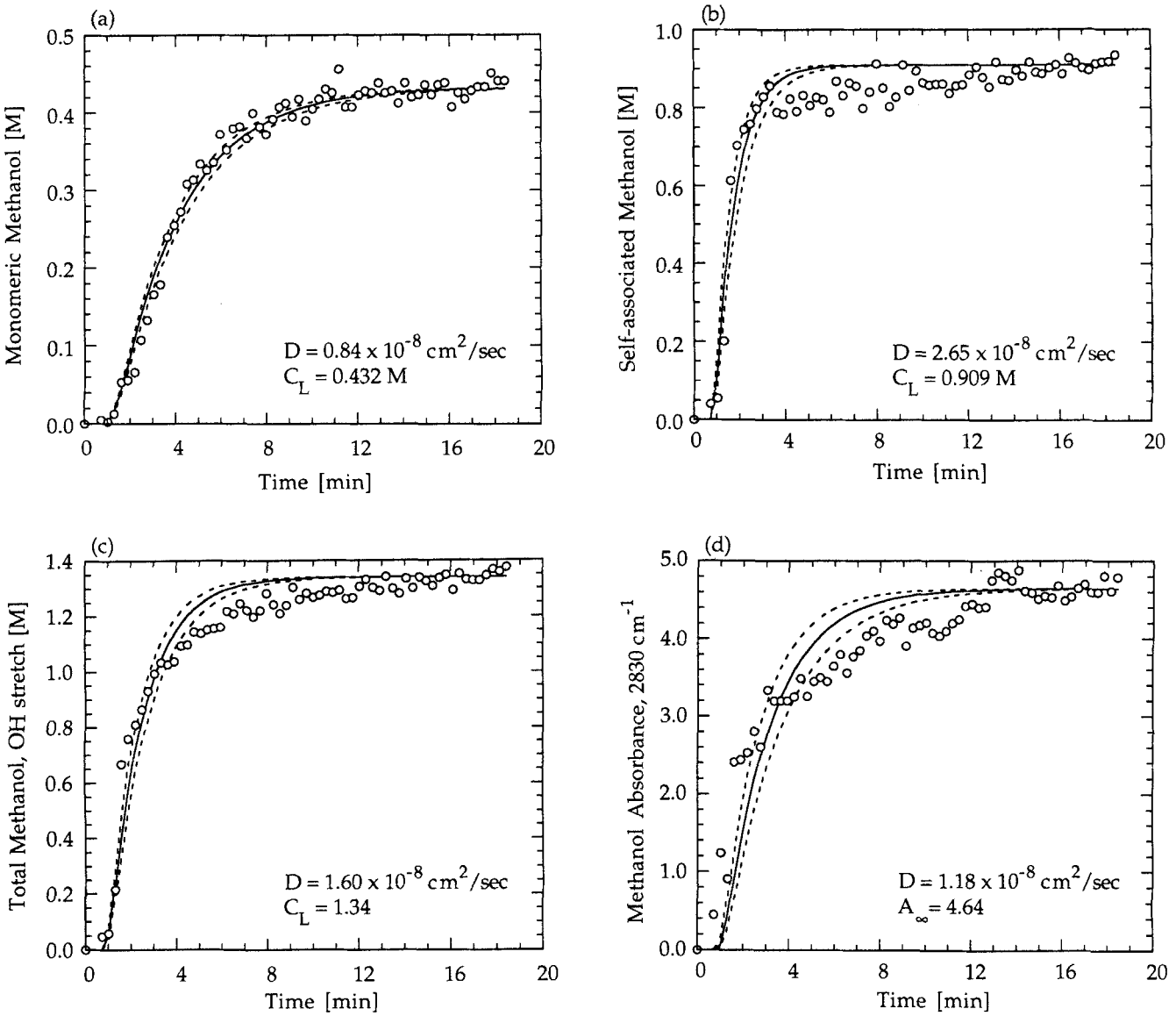

Figure 9. Integrated absorbance as a function of time for methanol diffusing in polystyrene at 23°C.

(a) Monomeric methanol (3,607 cm^{-1}); (b) self-associated methanol (3,350 cm^{-1}); (c) the sum of monomeric and self-associated methanol; (d) methyl CH absorbance of methanol (2,830 cm^{-1}). O experimental data; — FTIR-ATR Fickian diffusion model; --- 99% confidence intervals.

ied in two different experiments at different temperatures and sample thicknesses. The differences between these two experiments are noted in Table 1. Sample infrared spectra of methanol transport in PMMA for the second experiment at 35°C are shown in Figure 10. The presence of at least two distinct hydroxyl absorbances can be detected in the data, although the methanol peaks are neither widely nor distinctly separated, as in polystyrene. The total absorbance of methanol is estimated by integrating the entire hydroxyl stretching region, assuming a constant molar absorption coefficient. The dominance of the self-associated methanol peak at lower wave numbers in these spectra decreases the potential error in this approximation. The absorbance of methanol for both experiments, as a function of time, is plotted in Figure 11, where included also is the regressed fit of the simple FTIR-ATR Case II model (Eq. 10) to the experimental data. The calculated front velocity for the first experiment conducted at 20°C is 0.97×10^{-6} cm/s, while the velocity for the second experiment conducted at 35°C is 2.87×10^{-6} cm/s.

The diffusion of methanol in PMMA was positively identified as a Case II process. Even though a rather simplistic model of Case II diffusion was employed, this model fit both sets of experimental data well. More importantly, it was clear from this result that the FTIR-ATR technique was fully capable of discriminating between diffusion modes. The measured front velocity for the experiment conducted at 20°C is virtually identical to the front velocity of 1.0×10^{-6} cm/s reported by Grinsted et al. (1992) using nuclear magnetic resonance for methanol in PMMA at 25°C. The increase in velocity at a higher experimental temperature is consistent with

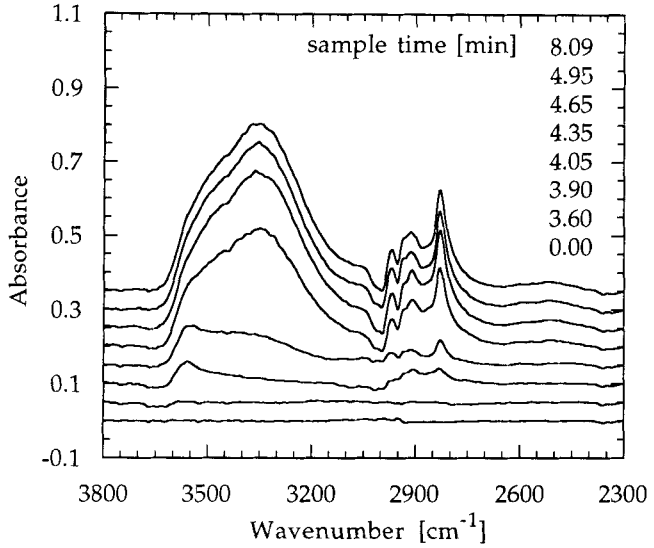

Figure 10. Infrared spectra of methanol transport in poly(methyl methacrylate) at 35°C.

the idea that the front velocity is dependent on the rate of chain relaxation. The characteristic relaxation time of polymers, which is inversely proportional to the relaxation rate, is known to decrease at increasing temperatures.

The detection of molecular interactions with FTIR-ATR spectroscopy also adds new information to the physical description of Case II diffusion. The presence of a precursor to the Case II front has long been suggested and experimentally observed in some systems (Gall et al., 1990). In the infrared spectra of methanol, the presence of measurable quantities of monomeric methanol at higher wavenumbers and preceding the main methanol peak is consistent with the hypothesis that the precursor is composed of penetrant that diffuses in advance of the swollen polymer front. These results suggest further lines of experimentation, where the relationship between the methanol concentration and the extent of hydrogen bonding can be used to obtain information about the polymer relaxation state during Case II diffusion.

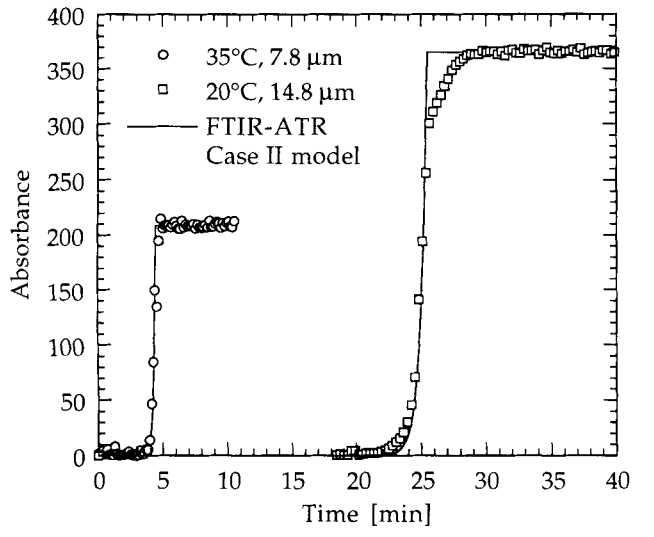

Figure 11. Integrated absorbance as a function of time for methanol transport in poly(methyl methacrylate) at 20 and 35°C.

Conclusions

FTIR-ATR spectroscopy, as applied to the study of diffusion in polymers, possesses several advantages over gravimetric sorption techniques. The greatest benefit, which is presently under investigation in our laboratory, is the ability to study multicomponent diffusion. Here, we have described a related benefit, the ability to study complex transport behavior in highly-interacting, single component diffusion. Infrared spectroscopy offers the potential to examine interactions between penetrants and polymers through shifts in the infrared spectrum. In many cases, FTIR-ATR spectroscopy is inherently more accurate than gravimetric sorption for the study of liquid penetrants because it is an *in situ* technique. Finally, it is possible to tailor experimental conditions such that data can be collected on convenient time scales, without compromising the quality of the results.

The formulation of the mathematical models that can be used to examine diffusion in FTIR-ATR spectroscopy is a straightforward procedure. The basic models for Fickian diffusion, with both a constant surface concentration and a mass-transfer boundary layer, were developed. Models for non-Fickian diffusion can also be prepared, as was demonstrated by the derivation of a simple FTIR-ATR model for Case II diffusion.

New experimental results were obtained for the diffusion of acetone in polypropylene and for methanol in polystyrene and poly(methyl methacrylate). The lack of existing data for these systems, and for many liquid penetrant-polymer systems, accents the utility of FTIR-ATR spectroscopy as a tool for analyzing diffusion in polymers. In addition to measuring systems that were previously difficult or unmeasurable, the results also introduce the ability to conduct advanced investigations of diffusion by exploiting the ability of infrared spectroscopy to measure specific interactions, such as hydrogen bonding. The ability to discriminate between diffusion modes and to employ non-Fickian diffusion models in FTIR-ATR spectroscopy was demonstrated by the measurement of Case II diffusion in the methanol-poly(methyl methacrylate) system.

Notation

A = absorbance at time t
A_∞ = absorbance at equilibrium
C = molar concentration of penetrant in the polymer film
C_b = molar concentration of penetrant in the bulk liquid
C_L = molar concentration of penetrant in the polymer at $z = L$
D = diffusion coefficient of the penetrant in the polymer
D_a = diffusion coefficient of the penetrant in the amorphous fraction
d_p = depth of penetration
E = magnitude of the electric field in the evanescent wave
E_0 = magnitude of the electric field at the polymer-IRE interface
$\mathcal{H}$ = Heaviside function
I = intensity of electric field
K = partition coefficient of penetrant between the polymer and liquid
k_c = liquid-phase mass-transfer coefficient
L = thickness of the polymer film

n_1 = refractive index of the polymer
n_2 = refractive index of the IRE
v = velocity of Case II diffusion front

Greek letters

α = boundary layer rate coefficient
β_n = parameters derived from boundary layer rate coefficient
γ = evanescent field decay coefficient
γ_∞ = value of γ at equilibrium
ϵ^* = lumped parameter incorporating molar extinction coefficient, number of reflections, cross-sectional area, and refractive indices
θ = angle of incidence of the internally reflected light
λ = wavelength of absorbed light
ϕ_a = amorphous fraction of polymer

Literature Cited

Adib, F., and P. Neogi, "Sorption with Oscillations in Solid Polymers," *AIChE J.*, **33**, 164 (1987).

Alfrey, T., Jr., E. F. Gurnee, and W. G. Lloyd, "Diffusion in Glassy Polymers," *J. Poly. Sci. Part C: Poly. Lett.*, **12**, 249 (1966).

Camera-Roda, G., and G. C. Sarti, "Mass Transport with Relaxation in Polymers," *AIChE J.*, **36**, 851 (1990).

Crank, J., *The Mathematics of Diffusion*, 2nd ed., Oxford University Press, Oxford (1975).

Fieldson, G. T., and T. A. Barbari, "The Use of FTi.r.-a.t.r. Spectroscopy to Characterize Penetrant Diffusion in Polymers," *Polymer*, **34**, 1146 (1993).

Gall, T. P., R. C. Lasky, and E. J. Kramer, "Case II Diffusion: Effect of Solvent Molecule Size," *Polymer*, **31**, 1491 (1990).

Grinsted, R. A., L. Clark, and J. L. Koenig, "Study of Cyclic Sorption-Desorption into Poly(methyl methacrylate) Rods Using NMR Imaging," *Macromol.*, **25**, 1235 (1992).

Jabbari, E., and N. A. Peppas, "The Use of ATR-FTIR to Study Interdiffusion in Polystyrene and Poly(vinyl methyl ether)," *Macromol.*, **26**, 2175 (1992).

Lustig, S. R., J. G. Van Alsten, and B. Hsiao, "Polymer Diffusion in Semicrystalline Polymers. 1. Poly(ether imide)/poly(aryl ether ketone ketone)," *Macromol.*, **26**, 3885 (1993).

Mirabella, F. M., Jr., ed., *Internal Reflection Spectroscopy: Theory and Applications*, Vol. 15, Marcel Dekker, New York (1993).

Neogi, P., "Anomalous Diffusion of Vapors through Solid Polymers," *AIChE J.*, **29**, 829 (1983).

Prausnitz, J. M., R. N. Lichtenthaler, and E. G. de Azevedo, *Molecular Thermodynamics of Fluid-Phase Equilibria*, 2nd ed., Prentice-Hall, Englewood Cliffs, NJ (1986).

Reilly, J. T., "Experimental Investigation of Acid-Base Interactions Using Fourier Transform Infrared (FT-IR) Spectroscopy," PhD Diss., The Johns Hopkins Univ. (1993).

Rogers, C. E., "Permeability of Gases and Vapors in Polymers," *Polymer Permeability*, J. Comyn, ed., Elsevier Applied Science, New York (1985).

Schlotter, N. E., and Y. P. Furlan, "Small Molecule Diffusion in Polyolefins Monitored Using the Infrared Evanescent Field," *Vib. Spectrosc.*, **3**, 147 (1992).

Sen, A., and M. Srivastava, *Regression Analysis: Theory, Methods and Applications*, Springer-Verlag, New York (1990).

Thomas, N. L., and A. H. Windle, "A Theory of Case II Diffusion," *Polymer*, **23**, 529 (1982).

Tompkin, H. G., "The Physical Basis for Analysis of the Depth of Absorbing Species Using Internal Reflection Spectroscopy," *Appl. Spectrosc.*, **28**, 335 (1974).

Van Alsten, J. G., and S. R. Lustig, "Polymer Mutual Diffusion Measurements Using Infrared ATR Spectroscopy," *Macromol.*, **25**, 5069 (1992).

Vieth, W. R., *Diffusion In and Through Polymers*, Oxford University Press, New York (1991).

Vorenkamp, E. J., J. van Ruiten, F. A. Kroesen, J. G. Meyer, J. Hoekstra, and G. Challa, "Interdiffusion and Adhesion of Poly(vinyl chloride) and Poly(methyl methacrylate)," *Poly. Commun.*, **30**, 116 (1989).

Windle, A. H., "Case II Sorption," *Polymer Permeability*, J. Comyn, ed., Elsevier Applied Science, New York (1985).

Manuscript received Mar. 18, 1994, and revision received May 13, 1994.